Conserved motifs on the cytoplasmic face of the protein translocation channel are critical for the transition between resting and active conformations

Received for publication, May 22, 2018, and in revised form, June 26, 2018 Published, Papers in Press, July 9, 2018, DOI 10.1074/jbc.RA118.004123

Elisabet C. Mandon, Cameron Butova[1], Amber Lachapelle[2], and Reid Gilmore[3]

From the Department of Biochemistry and Molecular Pharmacology, University of Massachusetts Medical School, Worcester, Massachusetts 01605

Edited by Phyllis I. Hanson

The Sec61 complex is the primary cotranslational protein translocation channel in yeast (*Saccharomyces cerevisiae*). The structural transition between the closed inactive conformation of the Sec61 complex and its open and active conformation is thought to be promoted by binding of the ribosome nascent-chain complex to the cytoplasmic surface of the Sec61 complex. Here, we have analyzed new yeast Sec61 mutants that selectively interfere with cotranslational translocation across the endoplasmic reticulum. We found that a single substitution at the junction between transmembrane segment TM7 and the L6/7 loop interferes with cotranslational translocation by uncoupling ribosome binding to the L6/7 loop from the separation of the lateral gate transmembrane spans. Substitutions replacing basic residues with acidic residues in the C-terminal tail of Sec61 had an unanticipated impact upon binding of ribosomes to the Sec61 complex. We found that similar charge-reversal mutations in the N-terminal tail and in cytoplasmic loop L2/3 did not alter ribosome binding but interfered with translocation channel gating. These findings indicated that these segments are important for the structural transition between the inactive and active conformations of the Sec61 complex. In summary our results have identified additional cytosolic segments of the Sec61 complex important for promoting the structural transition between the closed and open conformations of the complex. We conclude that positively charged residues in multiple cytosolic segments, as well as bulky hydrophobic residues in the L6/7–TM7 junction, are required for cotranslational translocation or integration of membrane proteins by the Sec61 complex.

Translocation of proteins across the yeast rough endoplasmic reticulum (RER)[4] can occur by cotranslational and post-translational pathways that utilize separate targeting and translocation machineries. Signal sequences of proteins that are cotranslationally translocated across the RER are more hydrophobic (1, 2) and are recognized by the signal recognition particle (SRP) as the nascent chain emerges from the polypeptide exit site on the large ribosomal subunit (3, 4). Targeting of SRP–ribosome nascent chain (RNC) complexes to the RER is mediated by the interaction between the SRP and the SRP receptor resulting in selective attachment of the RNC to the protein translocation channel (5, 6). The yeast Sec61 complex, which is composed of Sec61p, Sbh1p, and Sss1p, is the primary cotranslational protein translocation channel in yeast (7). Yeast Ssh1p, a homologue of Sec61p, assembles with Sbh2p and Sss1p to form a nonessential translocation channel that is specific for the cotranslational pathway (8–10).

In *Saccharomyces cerevisiae*, proteins that are translocated by the posttranslational pathway are thought to be delivered to the heptameric Sec complex by cytosolic chaperones and alternative targeting factors (2, 11, 12). The Sec complex is composed of the Sec61 heterotrimer plus the tetrameric Sec62/Sec63 complex (7, 13). Sec71p and Sec72p are fungi-specific subunits of the Sec62/Sec63 complex. The Sec complex, unlike the Sec61 or Ssh1 complexes, does not bind ribosomes directly (14). Ssh1p cannot replace Sec61p in the Sec complex (8), hence overexpression of Ssh1p cannot compensate for disruption of the essential *SEC61* gene or suppress the lethality caused by temperature-sensitive *sec61* alleles.

Ribosome profiling experiments using organelle-specific proximity labeling indicate that the majority of yeast secretome proteins, including previously identified substrates of the yeast posttranslational translocation pathway (1, 2), are translated in the vicinity of the rough endoplasmic reticulum (15). Ribosome profiling of endoplasmic reticulum (ER)–bound ribosome did not reveal a difference in distribution for ribosomes translating integral membrane proteins and secretory proteins in yeast (16). The latter observations led to the conclusion that yeast SRP is responsible for ER targeting of virtually all ribosomes

This work was supported by the NIGMS, National Institutes of Health Grant RO1 GM35687. The authors declare that they have no conflicts of interest with the contents of this article. The content is solely the responsibility of the authors and does not necessarily represent the official views of the National Institutes of Health.

This article contains Figure S1.

[1] Present address: Dept. of Biochemistry and Molecular Biology, University of Massachusetts Amherst, Amherst, MA 01003.

[2] Present address: Framingham Heart Study, Framingham, MA 01702.

[3] To whom correspondence should be addressed: 364 Plantation St. Worcester, MA 01605-2324. Tel.: 508-856-5894; Fax: 508-856-6464; E-mail: reid.gilmore@umassmed.edu.

[4] The abbreviations used are: RER, rough endoplasmic reticulum; AA, amino acid; CPY, carboxypeptidase Y; DPAPB, dipeptidylaminopeptidase B; ER, endoplasmic reticulum; OD, optical density; RNC, ribosome nascent chain; SD, synthetic minimal media containing dextrose; SEG, synthetic minimal media containing ethanol and glycerol; SR, signal recognition particle receptor; SRP, signal recognition particle; Ub, ubiquitin; UTA, ubiquitin translocation assay; YPAD, YPD containing adenine; YPAEG, YP media containing ethanol and glycerol as carbon sources supplemented with adenine; YPD, yeast extract, peptone, dextrose media.

synthesizing secretome proteins except for the tail-anchored membrane proteins that are targeted by the Get2 protein (17). However, rapid inactivation of yeast SRP combined with ER-specific ribosome profiling indicates that ribosomes synthesizing SRP-independent substrates remain ER-localized in SRP-deficient cells (18). In contrast, SRP-dependent secretome proteins including integral membrane proteins are mistargeted to the mitochondria in SRP-deficient cells (18).

Sec72p, which contains a tetratricopeptide repeat domain, can interact with both the cytosolic Hsp70 protein Ssa1p and the ribosome-bound Hsp70 protein Ssb1p (19). Mutagenesis of the Hsp70-binding sites in Sec72p revealed that these interactions contribute to targeting of nascent carboxypeptidase Y (CPY) to the Sec complex. Thus, Hsp70 binding to yeast secretome proteins that have less hydrophobic signal sequences may play a critical role in selective delivery of this class of secretome proteins to the Sec complex.

Structural insight into the Sec61 complex has been provided by X-ray crystal structures of archaebacterial SecYEβ (20, 21) and eubacterial SecYEG (22, 23). With respect to ribosome–Sec61 interactions, the structures show that the L6/7 and L8/9 cytosolic loops project well above the membrane surface. We had identified mutations in the L6/7 and the L8/9 loops of Sec61p that are critical for cotranslational protein translocation. Specifically, point mutations in cytosolic loop 6/7 (R275E) and loop 8/9 (R406E) of yeast Sec61p cause cotranslational translocation defects (24). The L8/9 segment is particularly critical for ribosome binding, as the R406E mutation in yeast Sec61p causes a complete block in binding of nontranslating ribosomes (24). Early cryo-EM structures of yeast and mammalian protein translocation complexes revealed three to four contact sites between the translating ribosome and the cytoplasmic face of the protein translocation channel (25, 26). The two major contact sites (C2 and C4) are near the polypeptide exit tunnel on the 60S ribosomal subunit and correspond to interactions between the 26S rRNA with cytoplasmic loops L6/7 and L8/9 of Sec61α. A more recent higher resolution structure of an RNC–Sec61 complex confirmed the location of L6/7 and L8/9 contact sites and revealed a single additional contact between the ribosome and the N terminus of Sec61γ (27). Thus, the existence of additional contact sites near the N terminus and C terminus of Sec61α (26) is now questioned. Notably, the N terminus of Sec61 (residues 1–23) and the C-terminal 10 residues of Sec61 (residues 467–476) were not resolved in several RNC–Sec61 complex structures (27, 28), so the distance between these potentially flexible segments of Sec61 and the ribosome is uncertain.

We have introduced point mutations that replace conserved basic residues with acidic residues in several cytoplasmically exposed segments of Sec61p to determine whether these regions of yeast Sec61 are important for the cotranslational translocation pathway. Charge-reversal substitutions in the C-terminal tail of Sec61 caused protein translocation defects and blocked ribosome binding when combined with the *sec61* R275E mutation in the L6/7 loop. Although charge-reversal substitutions in the N terminus and the L2/3 region caused cotranslational protein translocation defects, these point mutations did not have any impact on ribosome-binding activity. Instead, we propose that the N-terminal and L2/L3 mutations interfere with the transition between the inactive and active conformations of the Sec61 complex.

Results

Biochemical experiments (29) and more recent cryo-EM structures (26, 27) indicate that the 26S rRNA provides the major contact sites for Sec61 on the large ribosomal subunit. Charge-reversal substitutions in cytoplasmic loops L6/7 and L8/9 of Sec61 (*e.g.* R275E in L6/7 and R406E in L8/9) (Fig. 1, *A* and *B*) cause cotranslational translocation defects (24), which in the case of the *sec61* R406E allele can be explained by a complete block in 80S ribosome-binding activity. Despite the improved resolution of ribosome–Sec61 complex structures, it is unclear how RNC–Sec61 contacts promote the transition between the closed and open conformations.

Based on an alignment between the *Methanocaldococcus jannaschii* SecY sequence and a collection of 125 diverse eukaryotic Sec61 sequences (Fig. 1*C*), we identified conserved arginine and lysine residues in the N terminus (Arg-5 and Lys-11) and the C terminus (Lys-464 and Lys-470) of *S. cerevisiae* Sec61 (Fig. 1*A*, residues shown as *blue spheres*). It should be noted that a basic amino acid that aligns with *S. cerevisiae* Lys-470 is less well-conserved, yet roughly 40% of the Sec61 sequences we examined contain a basic residue in this vicinity in addition to the conserved basic residue that aligns with Lys-464. The conformation of the L2/3 loop differs markedly between the *M. jannaschii* SecYEβ crystal structure and cryo-EM structures of ribosome–Sec61 complexes (26–28). For that reason, we targeted conserved basic residues at the tip of the L2/L3 loop (Lys-108 Arg-111). We constructed three plasmids harboring pairs of charge-reversal substitutions (*sec61* R5E K11E, *sec61* K464E K470E, and *sec61* K108E R111E).

Regardless of the targeting pathway, insertion of the signal sequence into the signal sequence– binding site depends upon a partial separation of the lateral gate of the Sec61 complex which is composed of TM2, TM3, TM7, and TM8 of Sec61p (20). We also examined aligned Sec61 sequences at the junction between the L6/7 loop and TM7 and noticed several invariant bulky hydrophobic residues (Leu-285, Phe-286, Tyr-287) at this boundary (Fig. 1*C*, L6/7–TM7 junction). The *sec61* L285G mutant was constructed to test whether the enhanced flexibility expected from a glycine substitution at this site would interfere with lateral gate opening in response to RNC binding to the Sec61 complex (Fig. 1*B*).

Phenotypes of the charge-reversal sec61 mutants

Elimination of the auxiliary Ssh1 translocation channel causes a relatively minor decrease in cell growth rate (24). In contrast, disruption of genes encoding subunits of the SRP or the signal recognition particle receptor (SR) causes severe growth defects (30, 31) because of elimination of SRP-SR–mediated targeting of RNCs to the Sec61 complex. Consequently, *sec61* alleles can be identified which selectively interfere with the cotranslational protein translocation pathway by screening for mutations that cause growth and translocation defects in an *ssh1*Δ strain (24).

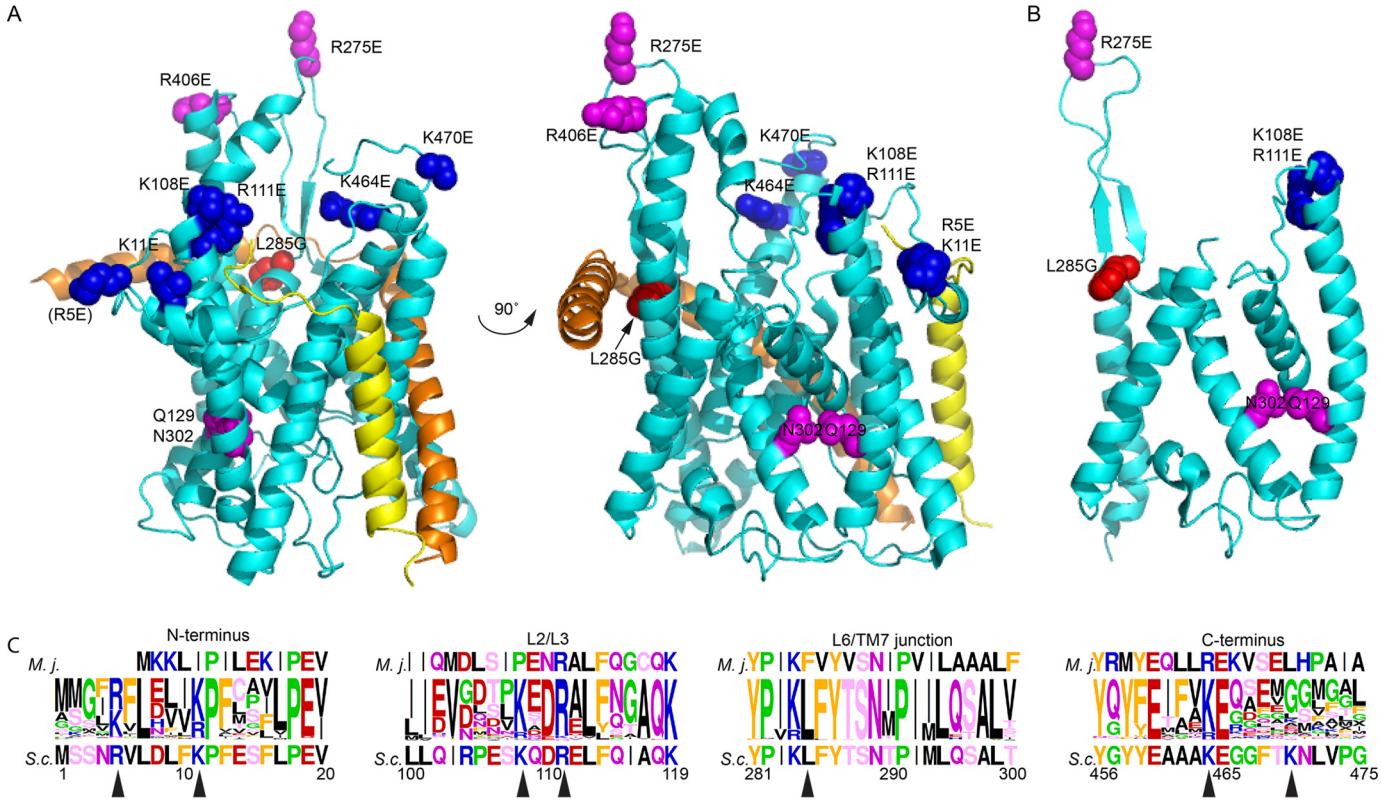

Figure 1. Location of yeast Sec61p residues selected for mutagenesis. *A* and *B*, the *M. jannaschii* SecYEβ channel (*A*) and lateral gate views (*B*) are color coded as follows: SecY (*cyan*), Secβ (*yellow*), SecE (*orange*), previously described mutants (*magenta*), new charge-reversal mutations (*blue*), and the L285G mutant (*red*). Conserved residues (Asn-302 and Gln-129) in the lateral gate polar cluster (36) that are important for channel gating are shown as *magenta spheres*. Sec61 residues selected for mutagenesis are mapped onto SecY based upon sequence alignment. The Sec61 R5E mutation is mapped onto M1 of *M. jannashii* SecY because *S. cerevisiae* Sec61 has a six-residue N-terminal extension relative to SecY. Residue numbers in all *panels* correspond to *S. cerevisiae* Sec61. *Panels A* and *B* were made using PYMOL v1.3 software and PDB ID 1RHZ. *C*, sequence logos for the N terminus, L2/3 and L6/TM7 junctions, and the C terminus of Sec61 were constructed by alignment of 125 diverse eukaryotic Sec61 sequences. Residues are color coded by side chain property; letter height is proportional to frequency. The *M. jannaschii* and *S. cerevisiae* sequences flank the logo. *Arrowheads* beneath the sequence logo designate residues selected for mutagenesis. Sequence logos were made using the website http://weblogo.berkeley.edu/logo.cgi.[5]

We replaced epitope-tagged Sec61 (Sec61–V5) with the untagged *sec61* mutants using a plasmid shuffle procedure in yeast strains that either express (*SSH1*) or do not express (*ssh1*Δ) Ssh1p, the pore-forming subunit of the auxiliary cotranslational protein translocation channel. The resulting yeast strains were maintained in synthetic media containing ethanol and glycerol (SEG) prior to conducting growth rate or protein translocation assays to minimize cellular adaptation to the Sec61p mutations and to prevent the accumulation of petite mutants. Yeast strains that lack the Ssh1p translocation channel display a 10–20% decrease in growth rate relative to a WT strain (8, 10) and are viable at both 30 and 37 °C when cultured on YPD plates (Fig. 2*A*). As shown previously (24), expression of the Ssh1p complex suppresses the growth defect of the positive control strain (*sec61* R275E R406E) at both temperatures (Fig. 2*A*). All four of the new *sec61* mutants displayed growth rate defects that were more severe at 37 °C than at 30 °C in the *ssh1*Δ background. Growth rate defects were comparable to that displayed by the previously characterized *sec61* R275E R406E mutant and were fully suppressed by the presence of the Ssh1p complex (Fig. 2*A*).

The observed growth rate defects are not because of reduced stable expression of the *sec61* mutant protein relative to WT Sec61p as protein immunoblots revealed only minor differences in Sec61p immunoreactivity between WT and mutant strains (Fig. S1). We can conclude that the *sec61* mutants are not misfolded as these *sec61* alleles are viable at 37 °C in the absence of the Ssh1p complex unlike the classical temperature-sensitive *sec61–2* allele (8). Secondly, *sec61* alleles that have folding defects (*e.g. sec61–2* and *sec61–3*) show obvious reductions in Sec61 expression at the permissive temperature (30 °C) (32, 33), and markedly lower Sec61 expression at the restrictive temperature because of proteasome-mediated degradation of Sec61 (32).

Integration of dipeptidylaminopeptidase B (DPAPB) and translocation of carboxypeptidase Y were monitored to detect defects in the cotranslational translocation pathway (DPAPB) and the posttranslational translocation pathway (CPY). The hydrophobicity of the signal sequence determines the targeting pathways and the translocation channel (Sec61 heterotrimer *versus* Sec complex) for these well-established assay substrates (1). The cells were transformed with a low-copy plasmid expressing DPAPB-HA under control of the GAPDH promoter to facilitate efficient labeling of DPAPB. Cells were shifted from SEG media into SD media and grown for 4 h prior to pulse labeling for 7 min with TRAN^{35}S-Label. Cotranslational integration of DPAPB into the ER membrane is detected by the electrophoretic mobility decrease that occurs upon addition of

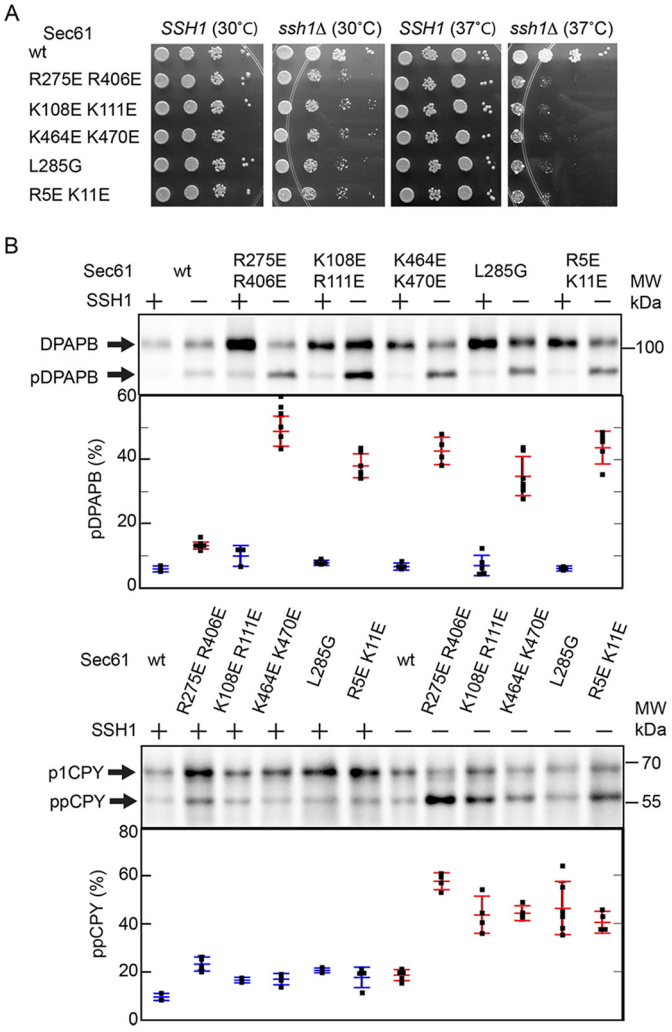

Figure 2. Ssh1p suppresses growth rate and protein translocation defects of the Sec61 cytoplasmic loop mutants. *A*, yeast strains (*SSH1* or *ssh1*Δ) that express WT or mutant alleles of Sec61p were maintained in SEG media prior to spotting onto YPAD plates to evaluate growth at 30 or 37 °C for 2 days. Please note that the spotting order for the second and third dilutions was inverted on the *SSH1* plate cultured at 37 °C. *B*, translocation assays of *sec61* mutants in *SSH1* or *ssh1*Δ strains. Yeast strains were shifted from SEG media into SD media and cultured for 4 h prior to pulse labeling. Integration of DPAPB and translocation of CPY was assayed by 7-min pulse labeling of WT and mutant yeast cells. CPY and DPAPB were immunoprecipitated from pulse-labeled cell extracts using CPY and DPAPB specific antisera. The glycosylated ER forms of CPY (p1) and DPAPB were resolved from nontranslocated precursors (ppCPY and pDPAPB) by SDS-PAGE. The percent integration (DPAPB) or translocation (CPY) is the average of two to eight determinations, one of which is shown here. *Blue* (*SSH1*) and *red* (*ssh1*Δ) *bars* represent mean and S.D. with individual data points plotted as *black squares*.

seven to eight *N*-linked oligosaccharides (Fig. 2*B*). The DPAPB precursor (pDPAPB) is slightly elevated in the *SEC61ssh1*Δ strain, but dramatically elevated in strains that lack Ssh1p and express a *sec61* mutant (Fig. 2*B*, *red error bars*). As observed previously for the *sec61* R275E R406E mutant (24), expression of the Ssh1p complex suppresses the translocation defects of the four new *sec61* mutants (Fig. 2*B*, *blue error bars*) consistent with the conclusion that Ssh1p is a cotranslational translocation channel (9, 10).

Translocation of CPY is detected by the addition of four *N*-linked oligosaccharides. Even though CPY is translocated through the Sec complex, which does not bind ribosomes (29), CPY translocation is reduced in the *sec61* R275E R406E mutant and in the new *sec61* mutants (Fig. 2*B*, *red error bars*). Expression of the Ssh1p complex suppresses the CPY translocation defect for all of the mutants (Fig. 2*B*, *blue error bars*), even though there are multiple lines of evidence that CPY is not translocated through the Ssh1p translocation channel but is instead exclusively translocated by the Sec complex. Translocation of CPY is completely blocked in yeast strains with nonconditional mutations in the Sec62/Sec63 complex (*sec62–101*, *sec63–201*), but as shown previously (24) and confirmed here, the CPY precursor is only slightly elevated in yeast strains lacking Ssh1p. Secondly, when SRP is inactivated (*sec65–1* mutant) (1) or when a subunit of the SRP or SR is depleted (1, 30, 31), CPY translocation is not inhibited, indicating that CPY translocation is not dependent on the SRP targeting pathway. Assays conducted using the split-ubiquitin system indicate that the CPY precursor is adjacent to Sec61p but not Ssh1p during translocation across the ER (9). Thus, as we proposed previously, the CPY translocation defect occurs by an indirect mechanism when cotranslational substrates like DPAPB transiently accumulate as aggregates in the cytosol (24).

Transient accumulation of cytosolic pDPAPB in ssh1Δsec61 mutants

Evidence for cytosolic accumulation of pDPAPB was obtained by protein immunoblotting. Total cell extracts were resolved by SDS-PAGE to detect the pDPAPB precursor at various time points after cells were shifted into the SD media (Fig. 3*A*). Quantification of protein immunoblots showed that maximal accumulation of pDPAPB in the *ssh1*Δ*sec61* mutants occurred 4–6 h after shift of the cells into the richer media (Fig. 3*B*, *black bars*). Levels of DPAPB precursor declined upon extended incubation, in most cases dropping below 15% pDPAPB after 24 h of culture compared with 4% pDPAPB for the *SEC61ssh1*Δ strain (Fig. 3*B*, *gray bars*). The decline in cytosolic pDPAPB is explained by an increase in the integration efficiency of DPAPB via a posttranslational pathway (24, 34), a reduction in total protein synthesis as the cells adapt to the defect in the cotranslational protein translocation pathway (35), and we presume by degradation of cytosolic pDPAPB aggregates. We have not tested whether degradation of the pDPAPB aggregates is sensitive to proteasome inhibitors. A second point to note is that the translocation defects for the *sec61* mutants were not additive in terms of accumulation of cytosolic pDPAPB (Fig. 3*B*). For example, the maximal accumulation of pDPAPB for the *sec61* R5E R11E K108E R111E mutant was higher than the value for the *sec61* R5E R11E mutant but lower than the value for the *sec61* K108E R111E mutants. These results indicate that the *sec61* mutations impact similar steps in cotranslational translocation, without causing a complete block in DPAPB integration when combined.

Ribosome binding to L6/L7 promotes lateral gate separation

The ribosomal contact site in L8/L9 is critical for ribosome binding to the Sec61 complex (24); contact sites in both L6/7 and L8/9 are necessary for efficient translocation channel gat-

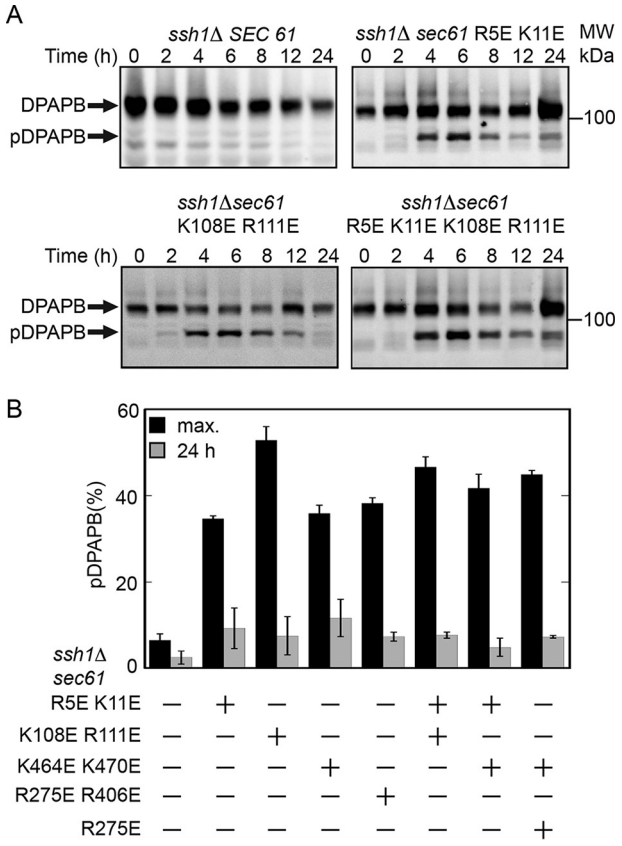

Figure 3. Transient accumulation of pDPAPB in *sec61* mutants cultured in S. D. media. Yeast strains were transferred from SEG media into liquid SD media and cultured at 30 °C for 0–24 h. *A*, total cell lysates from selected strains were resolved by SDS-PAGE to allow protein immunoblot detection of pDPAPB and DPAPB. *B*, DPAPB immunoblots including those displayed in *panel A* were quantified by densitometry to determine the maximal percent accumulation of pDPAPB (4 or 6 h time point) and the percent pDPAPB remaining at the 24 h time point. The quantified values are the average of two determinations. *Error bars* designate individual data points.

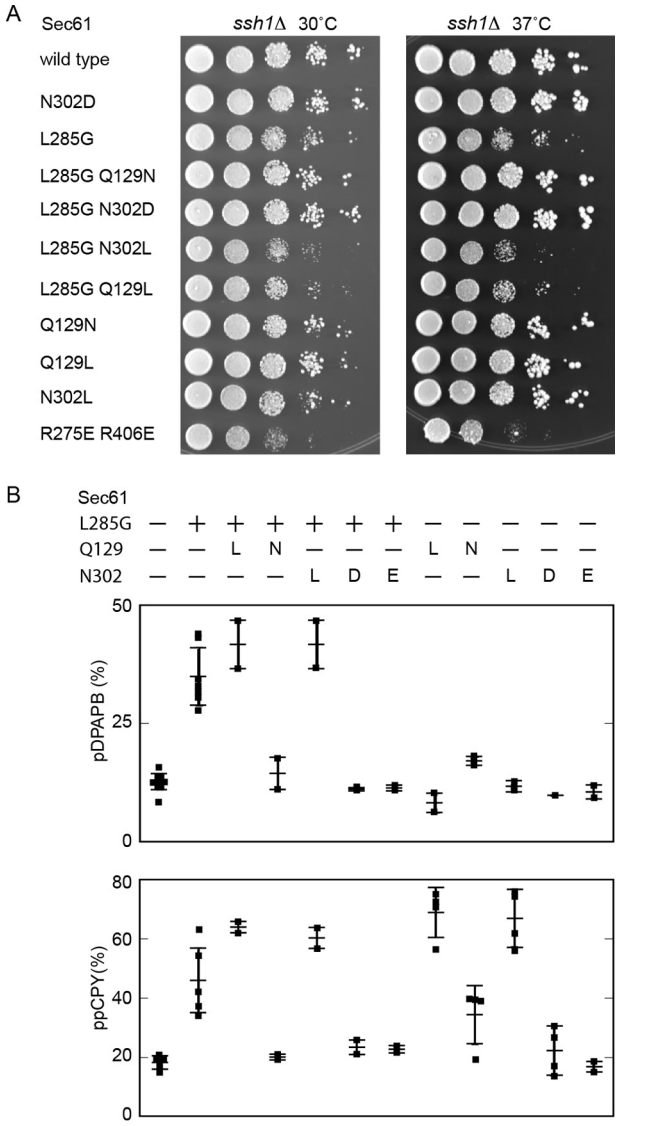

Figure 4. Interaction between *sec61* L285G and lateral gate polar cluster mutations. *A*, yeast strains that express WT or mutant alleles of Sec61p in the *ssh1*Δ background were maintained in SEG media prior to spotting onto YPAD plates to evaluate growth at 30 or 37 °C for 3 days. *B*, translocation assays of *sec61* mutants in *ssh1*Δ strains. Yeast strains were shifted from SEG media into SD media and cultured for 4 h prior to pulse labeling. Integration of DPAPB and translocation of CPY was assayed as in Fig. 2. The percent integration of DPAPB (*upper panel*) and translocation of CPY (*lower panel*) is the average of two to nine determinations. *Horizontal bars* designate mean and S.D.s, with individual data points plotted as *black squares*.

ing (34). The polar cluster in the lateral gate (Thr-87, Gln-129, and Asn-302) in *S. cerevisiae* links TM2 (Thr-87), TM3 (Gln-129), and TM7 (Asn-302). Insertion of a signal sequence into the signal sequence–binding site of Sec61 mandates the separation of the hydrogen bond network linking these residues. The polar cluster regulates lateral gate opening in response to the hydrophobicity of the signal sequence (36). The *sec61* L285G mutant was designed to test whether enhanced flexibility at the junction between L6/7 and TM7 would interfere with cotranslational translocation by weakening the structural link between the ribosome contact site in L6/7 and the lateral gate of the protein translocation channel. To explore this concept we constructed *sec61* double mutant strains that combine the L285G mutation with lateral gate polar cluster mutations that either stabilize the lateral gate (*sec61* Q129L, *sec61* N302L) and cause posttranslational protein translocation defects or mutations that destabilize the closed conformation of the lateral gate (*sec61* Q129N, *sec61* N302D, *sec61* N302E) and act as *sec61* prl alleles to promote translocation of substrates with signal sequence mutations (36).

Growth of strains that express the single and double *sec61* mutants was evaluated in the *ssh1*Δ background by colony dilution experiments (Fig. 4*A*). As reported previously (36), the *sec61* lateral gate polar cluster mutations do not cause growth rate defects at 30 or 37 °C (Fig. 4*A*). When combined with the L285G mutation, the Q129N and N302D mutations suppressed the growth rate defect caused by the L285G mutation at both 30° and 37 °C. The N302L and Q129L mutations did not suppress the growth rate defect when combined with the L285G (Fig. 4*A*).

The *sec61* single and double mutants were pulse-labeled 4 h after being shifted from SEG into SD media (Fig. 4*B*). Interestingly, the *sec61* L285G Q129N, *sec61* L285G N302D, and *sec61* L285G N302E mutants all lacked defects in the integration of DPAPB and translocation of CPY, indicating

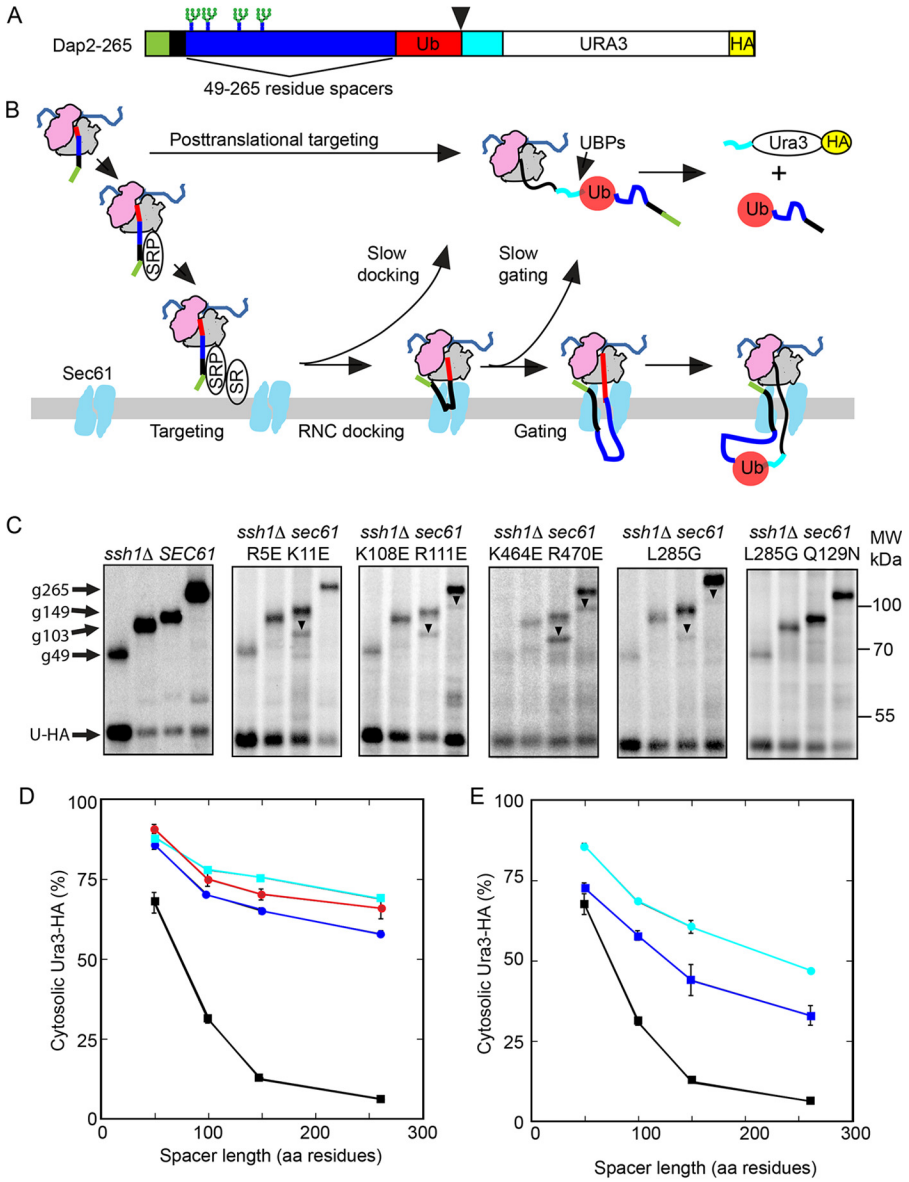

Figure 5. Translocon gating assays of *sec61* mutants. *A*, Dap2 reporters consist of i) the N-terminal cytoplasmic domain of Dap2p (*green*, $Dap2p_{1-29}$) followed by the TM span (*black*, $Dap2p_{30-45}$), ii) 49- to 265-residue spacer segments (*blue*) derived from Dap2p, iii) a Ub domain (*red*), iv) a 42-residue linker (*cyan*) with a processing site (*arrowhead*) for a Ub-specific protease, and v) a Ura3 reporter domain followed by a triple-HA epitope tag (*yellow*). Sites for *N*-linked glycosylation are indicated. *B*, cleavage of the Dap2 reporter defines the *in vivo* kinetics of translocon gating in *sec61* mutants. A delay in RNC docking or in channel gating allows folding of Ub in the cytosol and cleavage of the reporter to generate Ura3-HA. The color code for Dap2 segments is as defined in *panel A*. *C*, *in vivo* cleavage of the Dap2 reporter in *SEC61ssh1*Δ and *sec61ssh1*Δ mutant strains after 24 h of growth at 30 °C in SD media was evaluated by pulse labeling. Labels designate the intact glycosylated (*e.g. g49*) and cleaved (U-HA) reporter domains. *Downward-pointing arrowheads* in assays of mutant strains designate nonglycosylated intact reporters that correspond to cytosolic Dap2 reporter aggregates (10, 34). *D* and *E*, spacer-length dependence of Dap2 reporter cleavage (percent cytosolic Ura3-HA) for Sec61 WT (*D* and *E*, *black squares*), *sec61* R5E K11E (*D*, *blue circles*), *sec61* K108E R111E (*D*, *red circles*), *sec61* K464E K470E (*D*, *cyan squares*), *sec61* L285G (*E*, *cyan circles*), and *sec61* L285G Q129N (*E*, *blue squares*). Data points in *panels D* and *E* are averages of two experiments one of which is shown in *panel C*, with *error bars* designating individual data points. *Error bars* that are not visible are smaller than the data symbol.

that these prl alleles suppressed the translocation defect caused by the *sec61* L285G mutation. The *sec61* N302L and *sec61* Q129L mutants are not defective in the integration of the cotranslational substrate DPAPB as reported previously (36). However, these lateral gate stabilization mutations did not significantly alter the DPAPB integration defect of the *sec61* L285G mutant. The *sec61* L285G N302L and *sec61* L285G Q129L double mutants had a defect in CPY translocation that was similar to the parental *sec61* N302L and *sec61* Q129L mutants.

Translocation channel gating in sec61 mutants

The *in vivo* kinetics of DPAPB integration can be analyzed using the DAP2 series of ubiquitin (Ub) translocation assay (UTA) reporters (34, 37). The Dap2 reporters consist of the N-terminal cytosolic and transmembrane domains of DPAPB followed by a variable length spacer segment (49–265 residues) derived from the luminal domain of DPAPB, Ub, a cleavage site for a Ub-specific protease, and HA epitope–tagged Ura3p (Fig. 5*A*). Rapid folding of the Ub domain in the cytosol allows cleavage by a Ub-specific protease and release of the cleaved (Ura3-

HA) reporter segment (Fig. 5*B*). However, if Dap2–RNCs gate the translocon before the entire Ub domain emerges from the large ribosomal subunit, the intact reporter will be integrated into the ER. Mutations in SRP54 (37), SRα (34), and SRβ (10), or in the ribosome contact sites in L6/7 and L8/9 of Sec61 (34) retard reaction steps that precede translocon gating leading to elevated cleavage of the Dap2 series of UTA reporters. As the *ssh1*Δ *sec61* mutants do not have mutations in the SRP or SR subunit genes, any delays in translocation of the Dap2 UTA reporters can be ascribed to defects in the ribosome docking or translocon gating steps.

The *ssh1*Δ yeast strains expressing WT and mutant alleles of Sec61p were shifted from SEG media into SD media and cultured at 30 °C for 24 h prior to pulse labeling. Consequently, these assays monitor translocon gating by the Dap2 reporters after the adaptation process is complete as indicated by the reduced steady state levels of pDPAPB (Fig. 3). The intact glycosylated reporters (*e.g.* g49) as well as the cleaved Ura3-HA domain were recovered by immunoprecipitation with the anti-HA mAb. In *SEC61ssh1*Δ cells, Dap2 cleavage decreases as the spacer length is increased from 49 to 149 residues (Fig. 5, *C–E*, *black squares*), indicating that roughly 90% of Dap2-RNCs gate the translocon before 270 residues of the reporter emerge from the large ribosomal subunit (N terminus and TM span (45 AA) + spacer (149 AA) + Ub (76 AA) = 270 residues). Further increases in spacer length have little impact on Dap2 reporter cleavage in *SEC61 ssh1*Δ (Fig. 5*D*, *black squares*) with the plateau value (<10% Ura3–HA) for Dap265 cleavage corresponding to the fraction of the reporter that does not enter the cotranslational integration pathway.

Translocon gating assays of the new *sec61 ssh1*Δ mutants revealed elevated cleavage for all spacer lengths relative to WT cells (Fig. 5*C*). *Downward pointing arrowheads* in Fig. 5*C* designate nontranslocated, nonglycosylated intact reporters that are diagnostic of cytosolic Dap2 reporter aggregates (34). Of the three new double mutants, the *sec61* K464E K470E *ssh1*Δ mutant shows the greatest delay in translocation channel gating and the highest plateau value indicating that roughly 65% of the Dap2 reporters do not enter the cotranslational targeting pathway after adaptation (Fig. 5*D*, *cyan squares*). The adaptation process involves increased transcription of genes encoding cytoplasmic chaperones, and repression of gene products required for protein synthesis, thereby resulting in a reduced substrate load for the available protein translocation channels (35). The elevated plateau value for the *sec61* K464E K470E *ssh1*Δ mutant (Fig. 5*D*, *cyan squares*) is remarkably similar to what we had observed previously for the L6/7 (*sec61* R275E *ssh1*Δ) and L8/9 (*sec61* R406E *ssh1*Δ) mutants, also assayed after adaptation (34). Although the impact of the *sec61* R5E K11E *ssh1*Δ (Fig. 5, *C* and *D*, *blue circles*) and *sec61* K108E R111E *ssh1*Δ (Fig. 5, *C* and *D*, *red circles*) is not quite as dramatic, these assays indicate that translocon gating is strongly inhibited, and that the majority (55–65%) of the Dap2 reporters do not utilize the cotranslational pathway in these cells. The translocon gating assay for the *sec61* L285G *ssh1*Δ mutant showed a broader gating window, and a less well-defined plateau value indicating a delay in channel gating (Fig. 5, *C* and *E*, *cyan circles*). Although translocon gating by the *sec61* L285G Q129N *ssh1*Δ mutant (Fig. 5, *C* and *E*, *blue squares*) was improved relative to the *sec61* L285G *ssh1*Δ mutant, the prl mutation did not completely overcome the slow gating activity, nor did it redirect all of the Dap2-RNCs into a cotranslational translocation pathway. The *sec61* L285G N302D *ssh1*Δ and *sec61* L285G N302E *ssh1*Δ mutants were not tested using the translocon gating assay because of their similar behavior to the *sec61* L285G Q129N mutant in the pulse-labeling experiments.

Ribosome-binding activity of novel sec61 mutants

The L8/9 loop is particularly important for the stable interaction between a ribosome and the protein translocation channel as a single charge-reversal mutation in Sec61p (R406E) or in Ssh1p (R411E) is sufficient to block binding of a nontranslating ribosome to a translocation channel (24, 26). The L6/7 and L8/9 ribosome contact sites are evolutionarily conserved as these segments mediate contact between the 70S ribosome and *Escherichia coli* SecYEG (38). WT and mutant yeast Sec61 complexes were purified from strains expressing an affinity-tagged version of the Sbh1p subunit (His_6-FLAG-Sbh1p) of the Sec61 complex. Binding of the purified yeast Sec61 complexes to yeast ribosomes was evaluated by a centrifugation assay, wherein detection of bound or free Sec61 complexes in the supernatant and pellet fractions was achieved by protein immunoblot detection using anti-FLAG sera to detect Sbh1p. Sec61 complexes purified from *ssh1*Δ cells and from the *ssh1*Δ *sec61* R406E mutant, respectively, served as positive and negative controls for ribosome-binding activity (Fig. 6). WT Sec61 complexes remain in the supernatant fraction when ribosomes are absent but are quantitatively recovered in the pellet fraction when ribosomes are present in roughly 3-fold excess relative to the Sec61 complex. As reported previously, Sec61 complexes purified from the *sec61* R406E mutant lack detectable ribosome-binding activity under these conditions (24). Charge-reversal substitutions in the N terminus (*sec61* R5E KllE) and in the L2/3 loop (*sec61* K108E R111E) did not cause defects in binding of nontranslating ribosomes even when combined (Fig. 6, *upper panel*). The finding that the mutations in the C-terminal tail of Sec61p (*sec61* K464E K470E) did not reduce ribosome binding (Fig. 6, *lower panel*) was reminiscent of the previous evidence that a charge-reversal mutation in L6/7 loop (*sec61* R275E) does not inhibit ribosome-binding activity despite abundant structural evidence that the L6/7 loop of Sec61 makes direct contact with the 28S rRNA and eL39 in the large ribosomal subunit (26–28). We next asked whether a combination of the L6/7 and C-terminal point mutations would impact ribosome binding, and observed that the *sec61* R275E K464E K470E complex was recovered in the supernatant fraction in the presence or absence of ribosomes indicating that the combination of the L6/7 and C-terminal mutations block ribosome binding in a cooperative manner.

Previous reports have indicated the ribosome-Sec61 complex interaction has a high binding affinity (K_d ~5 nM) (14, 24, 29, 39). Under the conditions of our standard centrifugation assay where the ribosomes and Sec61 complexes are present at 40 nM and 13 nM respectively, a 2-fold decrease in ribosome-binding affinity would not be expected to cause an obvious reduction in the percentage of Sec61 that cosedimented with

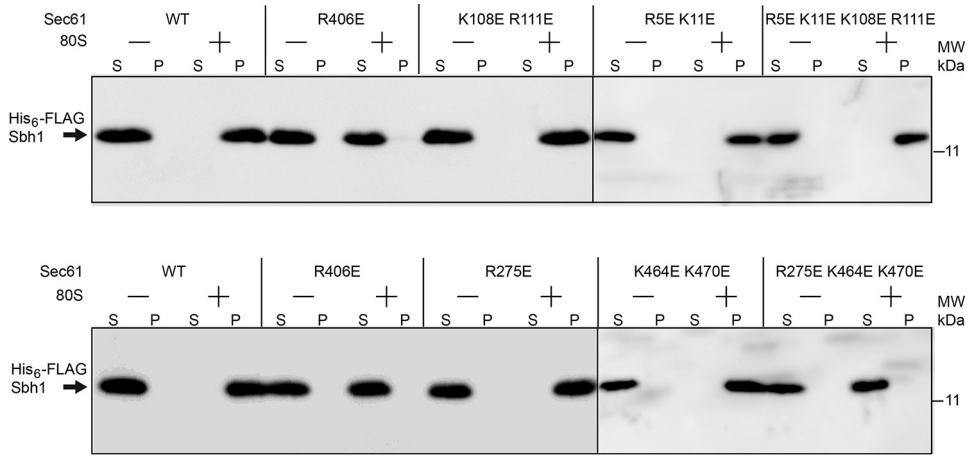

Figure 6. Ribosome-binding assays of *sec61* mutants. Purified WT and mutant Sec61 heterotrimers in detergent solution were incubated in the presence or absence of yeast 80S ribosomes prior to centrifugation to separate free Sec61 complexes in the supernatant fraction (*S*) from ribosome-bound Sec61 complexes in the pellet (*P*) fraction. Supernatant and pellet fractions were resolved by SDS-PAGE for protein immunoblot analysis using anti-FLAG to detect His_6-FLAG-Sbh1p. Each Sec61 preparation was assayed in two or more experiments, one of which is shown here. The *vertical lines* designate samples from the same experiment that were electrophoresed on separate gels.

the ribosomes. To address this caveat, additional assays of the WT, *sec61* R406E, *sec61* R275E, and *sec61* K464E K470E mutants were conducted using 4-fold lower concentrations of both 80S ribosomes and purified Sec61 complexes. Using these altered conditions, we were still unable to detect a ribosome-binding defect for the *sec61* R275E and the *sec61* K464E K470E mutants (data not shown).

Discussion

Analysis of yeast Sec61 cytosolic L6/7 and L8/9 mutants (24) and the subsequent cryo-EM of ribosome–Sec61 complexes (26–28) established that L6/7 and L8/9 form the primary contacts between a translating ribosome and the Sec61 complex. In this study we identified additional cytosolic segments of Sec61 that are important for promoting the structural transition between the closed and open conformations of the Sec61 complex. The mutations in the N-terminal segment, L2/L3 loop, C-terminal segment, and the L285G mutation all caused cotranslational specific translocation defects based upon the criteria established previously (24). The new *sec61* mutants could be suppressed by expression of the Ssh1p complex, and underwent an adaptation process that is exemplified by transient cytosolic accumulation of pDPAPB when cells are shifted from poor to rich media. Even after adaptation, the translocon gating assays revealed that translocation was abnormal, with the majority of DPAPB integration occurring by a posttranslational translocation pathway.

Our observations are consistent with the view that these new *sec61* point mutations interfere with the transition between the resting and active conformation of the protein translocation channel. A structural understanding of this transition has been obtained by comparing the crystal structure of *M. jannaschii* SecYEβ (20) with cryo-EM derived structures of translating and nontranslating 80S ribosomes bound to the mammalian Sec61 complex (27, 28). As there are distinct differences between all three structures, the SecYEβ structure corresponds to a closed/resting conformation, Sec61 bound to a nontranslating ribosome is thought to be in a primed conformation, whereas Sec61 bound to a ribosome translating a secretory protein is in an active or open conformation (27). The new *sec61* mutants we have described here could interfere with the transitions between the resting, primed, and active states of the translocation channel or they could somehow interfere with transport of the nascent polypeptide through the transport pore. The latter possibility is unlikely because the heptameric Sec complexes containing the new *sec61* alleles are fully functional for post-translational protein translocation of CPY in cells that express the auxiliary Ssh1p complex. As summarized earlier, the available evidence is that CPY is exclusively translocated through the Sec complex.

Despite the evidence that the L6/7 loop forms one of the primary contact sites with the large ribosomal subunit, the *sec61* R275E mutation does not prevent ribosome binding. The *sec61* R275E mutation causes a cotranslational protein translocation defect that is as severe as the *sec61* R406E mutation. Here, we found that ribosome binding is blocked when the R275E mutation is combined with the charge-reversal mutations in the C terminus (*sec61* K464E K470E). High-resolution cryoelectron microscope structures of Sec61–ribosome complexes do not reveal direct contacts between the C terminus of Sec61 and the ribosome as this segment of Sec61α is either unresolved (27) or is modeled as an extended chain that bends back toward the membrane surface (28). Given the apparent lack of direct contact between the C terminus of Sec61 and the ribosome in both the primed and active conformations, how can we account for the impact of the K464E K470E mutations on cotranslational protein translocation and ribosome-binding activity? One possibility is that the C terminus of Sec61 contacts the ribosome transiently during the transition between the inactive, primed, and active conformations of the Sec61–ribosome complex. A second possibility is that an interaction between the L6/7 and L8/9 loops and the ribosome is electrostatically perturbed by the K464E K470E mutations in the C terminus of Sec61p, thereby enhancing the negative impact of the R275E mutation on ribosome binding. A third possibility

would be that conformational flexibility of the C terminus of Sec61 is important for function. Further insight into the mechanism responsible for the translocation defect of the *sec61* K464E K470E mutant might be achieved by structural analysis of complexes between an 80S ribosome and the mutant Sec61 complex.

The N-terminal 24 residues of Sec61 are not resolved in the cryo-EM structures of the Sec61-ribosome complex, whereas the L2/3 loop is more than 15Å away from the 60S subunit (27, 28). As such, these sites are very unlikely to contact the ribosome at any stage during the translocation reaction. Structures of the Sec61-inactive ribosome complex indicate that the L2/L3 loop is altered relative to the structure of this loop in the SecYEβ crystal structure (20, 27, 28). Therefore, a conformational change in this loop may be necessary for the transition between the resting and primed states of the protein translocation channel. We hypothesize that the charge-reversal substitutions in the L2/L3 loop interfere with this conformational change resulting in the delay in translocon gating that was revealed by the UTA reporter assay. The absence of high-resolution structural information about the N terminus of Sec61 in the ribosome-Sec61 complex suggests that this region is disordered or can adopt multiple conformations, so it is unclear why the N-terminal charge-reversal substitutions cause a translocation defect.

The conformation of the L6/7 loop changes markedly between the resting and primed states (27). As reported by the Hegde lab (27), the L6/7 loop moves 11Å away from the L8/9 loop and rotates by 20–30Å, thereby altering the conformation of TM7, a lateral gate TM span. The lateral gate polar cluster residues (Gln-129 in TM3 and Asn-302 in TM7) are within hydrogen bond distance in the closed conformation of *M. jannaschii* SecY (Glu-122 and Asn-268), but are separated by roughly 10Å in the primed conformation of the Sec61–ribosome complex. Here, we tested whether a mutation (L285G) at the junction between L6/7 and TM7 would cause a protein translocation defect by weakening the structural link between the L6/7 loop and TM7. Indeed, the L285G mutation caused cell growth and protein translocation defects that could be suppressed by the presence of the Ssh1p complex. The observation that the L285G mutation does not cause a post-translational translocation defect when incorporated into the Sec complex suggests that rigidity of the L6/7–TM7 interface is less important for gating of the Sec complex, as the movement of the L6/7 loop is to accommodate the ribosome–nascent chain complex (27).

The translocon gating defect of the *sec61* L285G mutant was less severe than that displayed by the charge-reversal substitutions, and did not impact as high a percentage of Dap2 chains. Evidence that the L285G mutation impacts lateral gate opening was obtained by testing double mutants that combined the L285G mutation with polar cluster mutations that either stabilize (Q129L or N302L) or destabilize (Q129N, N302D, and N302E) the lateral gate. The lateral gate point mutants either suppressed (Q129N, N302D, and N302E) or exacerbated (Q129L, N302L) the growth rate defect of the L285G mutation. For the Q129N, N302D, and N302E mutations, the increased growth rate correlated with a suppression of the protein translocation defect and an increase in the percentage of Dap2 reporter chains that are translocated by the cotranslational translocation pathway as indicated by the translocon gating assay of the *sec61* L285G Q129N mutant.

Together our results reveal how positively charged residues in multiple cytosolic segments of Sec61 as well as the L6/7–TM7 junction are necessary for cotranslational translocation or integration of membrane proteins by the Sec61 complex. Prior to this work, there was no experimental evidence that the C terminus of Sec61 has an impact on protein translocation activity. Our results have also shed light on the poorly understood conformational differences of the L2/3 region of Sec61 that are observed upon comparison of the crystal structure of SecYEβ and the cryo-EM structures of Sec61-ribosome and Sec61-RNC complexes. The analysis of the L285G mutant provides mechanistic information linking the changes in conformation of the L6/7 loop upon RNC binding to the conformational changes that occur as the Sec61 complex transitions between the closed, primed, and active states.

Experimental procedures

Plasmid and strain construction

Standard yeast media (YPAD, YPAEG, SD, SEG), supplemented as noted, were used for growth and strain selection (40). To evaluate growth rates, yeast strains were cultured in SEG media (synthetic media supplemented with adenine, 2% ethanol, and 3% glycerol) at 30 °C to mid-log phase. After dilution of cells to 0.1 OD at 600 nm, 5 μl aliquots of 5-fold serial dilutions were spotted onto YPAD plates (YP media with adenine and dextrose) that were incubated at 30 or 37 °C for 2 days.

Oligonucleotides encoding amino acid substitutions were used as primers together with the template plasmid pBW11 (pRS315 *LEU2 SEC61*) (41) in recombinant PCR reactions to produce the *sec61* mutant alleles which were subcloned into the LEU2-marked low-copy plasmid pRS315 (42). The *sec61* mutants were characterized in *SSH1* (RGY402) and *ssh1*Δ yeast strains (RGY400) (24). A plasmid shuffle procedure (43) was used to replace the plasmid pEM324 (pRS316 *URA3 SEC61–V5*) with the LEU2-marked plasmids encoding the *sec61* mutants. Briefly, RGY400 and RGY402 were transformed with the pRS315 derivatives encoding mutant *sec61* alleles, and Leu$^+$ prototrophs were selected on SD (synthetic defined media with dextrose) plates supplemented with adenine, tryptophan, and uracil. Several transformants for each *sec61* mutant were streaked onto plates containing 5-fluoro-orotic acid (5-FOA) and grown for 2 d at 30 °C to select for colonies that had lost the pEM324 plasmid. Yeast *sec61* mutants were maintained on SEG media (synthetic minimal media containing 2% ethanol and 3% glycerol) to select against petite (ρ-) cells.

Immunoprecipitation of radiolabeled proteins

Yeast strains expressing *sec61* mutants were transformed with the URA3-marked plasmid pDN317 encoding DPAPB-HA under control of the glyceraldehyde 3-phosphate dehydrogenase promoter (1, 7, 24). After growth at 30 °C in SEG media to mid-log phase (0.2 to 0.6 OD at 600 nm) yeast were collected by centrifugation and resuspended in SD media and grown for 4 h at 30 °C. Yeast cells were collected by centrifugation and

resuspended in fresh SD media at a density of 6 A_{600}/ml and pulse-labeled for 7 min with TRAN-^{35}S-Label (100 μCi/OD). Radiolabeling experiments were terminated by dilution of the culture with an equal volume of ice-cold 20 mM NaN_3, followed by freezing in liquid nitrogen. Rapid lysis of cells with glass beads and immunoprecipitation of yeast proteins was done as described (44). Immunoprecipitated proteins were resolved by SDS-PAGE. Dry gels were exposed to a phosphor screen, scanned in Typhoon FLA 9000 (GE Healthcare), and quantified using AlphaEaseFC.

Total protein extracts were prepared as described (45) from cells after 0–24 h of growth at 30 °C in SD media. Proteins were resolved by SDS-PAGE, transferred to PVDF membranes, and incubated with anti-DPAPB sera. Peroxidase-labeled second antibodies were visualized using an ECL Western blotting detection kit (Amersham Biosciences).

Rabbit polyclonal antibodies to yeast CPY and DPAPB were described previously (24, 46). Rabbit polyclonal antibodies to yeast Sec61 were described previously (47) and were provided by Dr. Randy Schekman (University of California, Berkeley). The mouse mAb to PGK (no. 45920) was obtained from Thermo Fisher Scientific. The mouse monoclonal anti-HA antibody (11867423001) was from Roche. The mouse monoclonal anti-DDK (F3165 anti-FLAG M2) was obtained from Sigma-Aldrich.

Ubiquitin translocation assay (UTA)

The Dap2 series of UTA reporters (Dap2–49 to -265) has been described previously (34). Cells expressing Dap2 reporters were radiolabeled with TRAN^{35}S-Label as described above. The intact reporters and the Ura3-HA fragments were immunoprecipitated with anti-HA monoclonal antibodies. The distribution of methionine and cysteine residues in the intact UTA reporter and the Ura3-HA fragment was determined and the cleavage percentage was calculated as described (34).

Ribosome binding to purified Sec61 heterotrimers

Ribosomes were isolated from WT yeast as described (24, 48) and centrifuged through a high-salt sucrose cushion as described (24) to remove loosely associated proteins. Purification of the Sec61 complex was facilitated by construction of a strain (RGY404) that expresses His_6-FLAG-Sbh1p (24). The plasmid shuffle procedure was repeated to allow purification of the mutant Sec61 complexes from RGY404 derivatives. Sec61 complexes were purified from digitonin-solubilized yeast microsomes by sequential chromatography on Con-A Sepharose, Ni-NTA Agarose, Q Sepharose Fast Flow, and SP Sepharose Fast Flow as previously described (7, 24). The cosedimentation assay to measure binding of purified Sec61p heterotrimers to ribosomes in detergent solution was performed as described (29). 300 fmol of yeast ribosomes were preincubated with 100 fmol of purified Sec61 complexes in a total volume of 7.5 μl. Ribosome–Sec61 complexes were separated from free ribosomes by centrifugation. Sec61 complexes in the pellet and supernatant fractions were detected using anti-FLAG sera to detect His_6-FLAG-Sbh1p.

Bioinformatics analysis and generation of sequence logos

Eukaryotic Sec61 sequences were retrieved from the NCBI database by searching for Sec61 and saving no more than a single sequence from a genus. Sequence logos were constructed using 125 Sec61 sequences from diverse eukaryotes using the website http://weblogo.berkeley.edu/logo.cgi.[5]

Author contributions—E. C. M. and R. G. conceptualization; E. C. M., C. B., and A. L. investigation; E. C. M., C. B., and R. G. writing-review and editing; R. G. supervision; R. G. funding acquisition; R. G. writing-original draft; R. G. project administration.

Acknowledgments—We thank Randy Schekman for the anti-Sec61p antisera.

References

1. Ng, D. T. W., Brown, J. D., and Walter, P. (1996) Signal sequences specify the targeting route to the endoplasmic reticulum. *J. Cell Biol.* **134,** 269–278 CrossRef Medline
2. Ast, T., Cohen, G., and Schuldiner, M. (2013) A network of cytosolic factors targets SRP-independent proteins to the endoplasmic reticulum. *Cell* **152,** 1134–1145 CrossRef Medline
3. Walter, P., and Johnson, A. E. (1994) Signal sequence recognition and protein targeting to the endoplasmic reticulum membrane. *Ann. Rev. Cell Biol.* **10,** 87–119 CrossRef Medline
4. Halic, M., Becker, T., Pool, M. R., Spahn, C. M., Grassucci, R. A., Frank, J., and Beckmann, R. (2004) Structure of the signal recognition particle interacting with the elongation-arrested ribosome. *Nature* **427,** 808–814 CrossRef Medline
5. Song, W., Raden, D., Mandon, E. C., and Gilmore, R. (2000) Role of Sec61α in the regulated transfer of the ribosome-nascent chain complex from the signal recognition particle to the translocation channel. *Cell* **100,** 333–343 CrossRef Medline
6. Zhang, X., Rashid, R., Wang, K., and Shan, S. O. (2010) Sequential checkpoints govern substrate selection during cotranslational protein targeting. *Science* **328,** 757–760 CrossRef Medline
7. Panzner, S., Dreier, L., Hartmann, E., Kostka, S., and Rapoport, T. A. (1995) Posttranslational protein transport in yeast reconstituted with a purified complex of Sec proteins and Kar2p. *Cell* **81,** 561–570 CrossRef Medline
8. Finke, K., Plath, K., Panzer, S., Prehn, S., Rapoport, T. A., Hartmann, E., and Sommer, T. (1996) A second trimeric complex containing homologs of the Sec61p complex functions in protein transport across the ER membrane of *S. cerevisiae*. *EMBO J.* **15,** 1482–1494 Medline
9. Wittke, S., Dünnwald, M., Albertsen, M., and Johnsson, N. (2002) Recognition of a subset of signal sequences by Ssh1p, a Sec61p-related protein in the membrane of endoplasmic reticulum of yeast *Saccharomyces cerevisiae*. *Mol. Biol. Cell* **13,** 2223–2232 CrossRef Medline
10. Jiang, Y., Cheng, Z., Mandon, E. C., and Gilmore, R. (2008) An interaction between the SRP receptor and the translocon is critical during cotranslational protein translocation. *J. Cell Biol.* **180,** 1149–1161 CrossRef Medline
11. Corsi, A. K., and Schekman, R. (1996) Mechanism of polypeptide translocation into the endoplasmic reticulum. *J. Biol. Chem.* **271,** 30299–30302 CrossRef Medline
12. Aviram, N., Ast, T., Costa, E. A., Arakel, E. C., Chuartzman, S. G., Jan, C. H., Haßdenteufel, S., Dudek, J., Jung, M., Schorr, S., Zimmermann, R., Schwappach, B., Weissman, J. S., and Schuldiner, M. (2016) The SND proteins constitute an alternative targeting route to the endoplasmic reticulum. *Nature* **540,** 134–138 CrossRef Medline

[5] Please note that the JBC is not responsible for the long-term archiving and maintenance of this site or any other third party hosted site.

13. Deshaies, R. J., Sanders, S. L., Feldheim, D. A., and Schekman, R. (1991) Assembly of yeast Sec proteins involved in translocation into the endoplasmic reticulum into a membrane-bound multisubunit complex. *Nature* **349,** 806–808 CrossRef Medline
14. Prinz, A., Hartmann, E., and Kalies, K. U. (2000) Sec61p is the main ribosome receptor in the endoplasmic reticulum of *Saccharomyces cerevisiae*. *Biol. Chem.* **381,** 1025–1029 CrossRef Medline
15. Jan, C. H., Williams, C. C., and Weissman, J. S. (2014) Principles of ER cotranslational translocation revealed by proximity-specific ribosome profiling. *Science* 346, 1257521 CrossRef Medline
16. Chartron, J. W., Hunt, K. C., and Frydman, J. (2016) Cotranslational signal-independent SRP preloading during membrane targeting. *Nature* **536,** 224–228 CrossRef Medline
17. del Alamo, M., Hogan, D. J., Pechmann, S., Albanese, V., Brown, P. O., and Frydman, J. (2011) Defining the specificity of cotranslationally acting chaperones by systematic analysis of mRNAs associated with ribosome-nascent chain complexes. *PLoS Biol.* **9,** e1001100 CrossRef Medline
18. Costa, E. A., Subramanian, K., Nunnari, J., and Weissman, J. S. (2018) Defining the physiological role of SRP in protein-targeting efficiency and specificity. *Science* **359,** 689–692 CrossRef Medline
19. Tripathi, A., Mandon, E. C., Gilmore, R., and Rapoport, T. A. (2017) Two alternative binding mechanisms connect the protein translocation Sec71-Sec72 complex with heat shock proteins. *J. Biol. Chem.* **292,** 8007–8018 CrossRef Medline
20. Van den Berg, B., Clemons, W. M., Jr., Collinson, I., Modis, Y., Hartmann, E., Harrison, S. C., and Rapoport, T. A. (2004) X-ray structure of a protein-conducting channel. *Nature* **427,** 36–44 CrossRef Medline
21. Egea, P. F., and Stroud, R. M. (2010) Lateral opening of a translocon upon entry of protein suggests the mechanism of insertion into membranes. *Proc. Natl. Acad. Sci. U.S.A.* **107,** 17182–17187 CrossRef Medline
22. Zimmer, J., Nam, Y., and Rapoport, T. A. (2008) Structure of a complex of the ATPase SecA and the protein-translocation channel. *Nature* **455,** 936–943 CrossRef Medline
23. Tsukazaki, T., Mori, H., Fukai, S., Ishitani, R., Mori, T., Dohmae, N., Perederina, A., Sugita, Y., Vassylyev, D. G., Ito, K., and Nureki, O. (2008) Conformational transition of Sec machinery inferred from bacterial SecYE structures. *Nature* **455,** 988–991 CrossRef Medline
24. Cheng, Z., Jiang, Y., Mandon, E. C., and Gilmore, R. (2005) Identification of cytoplasmic residues of Sec61p involved in ribosome binding and cotranslational translocation. *J. Cell Biol.* **168,** 67–77 CrossRef Medline
25. Ménétret, J. F., Hegde, R. S., Aguiar, M., Gygi, S. P., Park, E., Rapoport, T. A., and Akey, C. W. (2008) Single copies of Sec61 and TRAP associate with a nontranslating mammalian ribosome. *Structure* **16,** 1126–1137 CrossRef Medline
26. Becker, T., Bhushan, S., Jarasch, A., Armache, J. P., Funes, S., Jossinet, F., Gumbart, J., Mielke, T., Berninghausen, O., Schulten, K., Westhof, E., Gilmore, R., Mandon, E. C., and Beckmann, R. (2009) Structure of monomeric yeast and mammalian Sec61 complexes interacting with the translating ribosome. *Science* **326,** 1369–1373 CrossRef Medline
27. Voorhees, R. M., Fernández, I. S., Scheres, S. H., and Hegde, R. S. (2014) Structure of the mammalian ribosome-Sec61 complex to 3.4 Å resolution. *Cell* **157,** 1632–1643 CrossRef Medline
28. Gogala, M., Becker, T., Beatrix, B., Armache, J. P., Barrio-Garcia, C., Berninghausen, O., and Beckmann, R. (2014) Structures of the Sec61 complex engaged in nascent peptide translocation or membrane insertion. *Nature* **506,** 107–110 CrossRef Medline
29. Prinz, A., Behrens, C., Rapoport, T. A., Hartmann, E., and Kalies, K. U. (2000) Evolutionarily conserved binding of ribosomes to the translocation channel via the large ribosomal RNA. *EMBO J.* **19,** 1900–1906 CrossRef Medline
30. Ogg, S. C., Poritz, M. A., and Walter, P. (1992) Signal recognition particle receptor is important for cell growth and protein secretion in *Saccharomyces cerevisiae*. *Mol. Biol. Cell* **3,** 895–911 CrossRef Medline
31. Hann, B. C., and Walter, P. (1991) The signal recognition particle in *S. cerevisiae*. *Cell* **67,** 131–144
32. Biederer, T., Volkwein, C., and Sommer, T. (1996) Degradation of subunits of the Sec61p complex, an integral component of the ER membrane, by the ubiquitin-proteasome pathway. *EMBO J.* **15,** 2069–2076 Medline
33. Trueman, S. F., Mandon, E. C., and Gilmore, R. (2011) Translocation channel gating kinetics balances protein translocation efficiency with signal sequence recognition fidelity. *Mol. Biol. Cell* **22,** 2983–2993 CrossRef Medline
34. Cheng, Z., and Gilmore, R. (2006) Slow translocon gating causes cytosolic exposure of transmembrane and lumenal domains during membrane protein integration. *Nat. Struct. Mol. Biol.* **13,** 930–936 CrossRef Medline
35. Mutka, S. C., and Walter, P. (2001) Multifaceted physiological response allows yeast to adapt to the loss of the signal recognition particle-dependent protein-targeting pathway. *Mol. Biol. Cell* **12,** 577–588 CrossRef Medline
36. Trueman, S. F., Mandon, E. C., and Gilmore, R. (2012) A gating motif in the translocation channel sets the hydrophobicity threshold for signal sequence function. *J. Cell Biol.* **199,** 907–918 CrossRef Medline
37. Johnsson, N., and Varshavsky, A. (1994) Ubiquitin-assisted dissection of protein transport across membranes. *EMBO J.* **13,** 2686–2698 Medline
38. Ménétret, J. F., Schaletzky, J., Clemons, W. M., Jr., Osborne, A. R., Skånland, S. S., Denison, C., Gygi, S. P., Kirkpatrick, D. S., Park, E., Ludtke, S. J., Rapoport, T. A., and Akey, C. W. (2007) Ribosome binding of a single copy of the SecY complex: Implications for protein translocation. *Mol. Cell* **28,** 1083–1092 CrossRef Medline
39. Raden, D., Song, W., and Gilmore, R. (2000) Role of the cytoplasmic segments of Sec61α in the ribosome-binding and translocation-promoting activities of the Sec61 complex. *J. Cell Biol.* **150,** 53–64 CrossRef Medline
40. Sherman, F. (1991) Getting started with yeast. *Methods Enzymol.* **194,** 3–21 CrossRef Medline
41. Wilkinson, B. M., Critchley, A. J., and Stirling, C. J. (1996) Determination of the transmembrane topology of yeast Sec61p; an essential component of the ER translocation complex. *J. Biol. Chem.* **271,** 25590–25597 CrossRef Medline
42. Sikorski, R. S., and Hieter, P. (1989) A system of shuttle vectors and yeast host strains designed for efficient manipulation of DNA in *Saccharomyces cerevisiae*. *Genetics* **122,** 19–27 Medline
43. Sikorski, R. S., and Boeke, J. D. (1991) *In vitro* mutagenesis and plasmid shuffling: From cloned genes to mutant yeast. *Methods Enzymol.* **194,** 302–318
44. Rothblatt, J., and Schekman, R. (1989) A hitchhiker's guide to the analysis of the secretory pathway in yeast. *Methods Cell Biol.* **32,** 3–36 CrossRef Medline
45. Arnold, C. E., and Wittrup, K. D. (1994) The stress response to loss of signal recognition particle function in *Saccharomyces cerevisiae*. *J. Biol. Chem.* **269,** 30412–30418 Medline
46. Silberstein, S., Collins, P. G., Kelleher, D. J., and Gilmore, R. (1995) The essential OST2 gene encodes the 16-kD subunit of the yeast oligosaccharyltransferase, a highly conserved protein expressed in diverse eukaryotic organisms. *J. Cell Biol.* **131,** 371–383 CrossRef Medline
47. Stirling, C. J., Rothblatt, J., Hosobuchi, M., Deshaies, R., and Schekman, R. (1992) Protein translocation mutants defective in the insertion of integral membrane proteins into the endoplasmic reticulum. *Mol. Biol. Cell* **3,** 129–142 CrossRef Medline
48. Beckmann, R., Bubeck, D., Grassucci, R., Penczek, P., Verschoor, A., Blobel, G., and Frank, J. (1997) Alignment of conduits for the nascent polypeptide chain in the ribosome-Sec61 complex. *Science* **278,** 2123–2126 CrossRef Medline